AD-A281 526

T · H · E
OHIO
STATE
UNIVERSITY

Wing-Body Juncture Flows

Richard J. Bodonyi
Department of Aeronautical & Astronautical Engineering

DTIC
S **ELECTE**
JUL 1 4 1994
G **D**

January 1994

94-21213

94 7 11 497

REPORT DOCUMENTATION PAGE

Public reporting burden for this collection of information is estimated to average 1 hour per response, including the time for reviewing instructions, searching existing data sources, gathering and maintaining the data needed, and completing and reviewing the collection of information. Send comments regarding this burden estimate or any other aspect of this collection of information, including suggestions for reducing this burden, to Washington Headquarters Services, Directorate for Information Operations and Reports, 1215 Jefferson Davis Highway, Suite 1204, Arlington, VA 22202-4302, and to the Office of Management and Budget, Paperwork Reduction Project (0704-0188), Washington, DC 20503

1. AGENCY USE ONLY (Leave blank)	2. REPORT DATE Jan 94	3. REPORT TYPE AND DATES COVERED Final 1 Aug 90–31 Dec 93

4. TITLE AND SUBTITLE

Wing-Body Juncture Flows

5. FUNDING NUMBERS

DAAL03-90-G-0186

6. AUTHOR(S)

Richard J. Bodonyi

7. PERFORMING ORGANIZATION NAME(S) AND ADDRESS(ES)

Ohio State Univeristy
Columbus, Ohio 43210

8. PERFORMING ORGANIZATION REPORT NUMBER

9. SPONSORING/MONITORING AGENCY NAME(S) AND ADDRESS(ES)

U.S. Army Research Office
P.O. Box 12211
Research Triangle Park, NC 27709-2211

10. SPONSORING/MONITORING AGENCY REPORT NUMBER

ARO 28249.2-EG

11. SUPPLEMENTARY NOTES

The views, opinions and/or findings contained in this report are those of the author(s) and should not be construed as an official Department of the Army position, policy, or decision, unless so designated by other documentation.

12a. DISTRIBUTION/AVAILABILITY STATEMENT

Approved for public release; distribution unlimited.

12b. DISTRIBUTION CODE

13. ABSTRACT (Maximum 200 words)

Researchers have considered the flow structure near a small-scale wing-body combination within the framework of triple-deck theory. Thin airfoil theory was used to obtain the pressure distribution around a wing which in turn triggers a viscous-inviscid interaction near the wing-body juncture. As part of the formulation of the problem they have followed the lead of Smith & Gajjar (1984), utilizing the concept of an "effective hump shape" in the formulation of the nonlinear problem. This technique not only simplifies the pressure expression but also enhances the convergence of the numerical scheme even though the concept itself is just a transformation to convert the wing-body problem into a more conventional problem for computational efficiency.

14. SUBJECT TERMS		15. NUMBER OF PAGES 40
Airfoil Theory Boundary Layers Wing Body Juncture Flows Vortex Flow Wing-Body Problem		16. PRICE CODE

17. SECURITY CLASSIFICATION OF REPORT	18. SECURITY CLASSIFICATION OF THIS PAGE	19. SECURITY CLASSIFICATION OF ABSTRACT	20. LIMITATION OF ABSTRACT
UNCLASSIFIED	UNCLASSIFIED	UNCLASSIFIED	UL

NSN 7540-01-280-5500

Wing-Body Juncture Flows

Richard J. Bodonyi
Department of Aeronautical & Astronautical Engineering

January 1994

Accesion For		
NTIS CRA&I		☑
DTIC TAB		☐
Unannounced		☐
Justification		
By		
Distribution /		
Availability Codes		
Dist	Avail and / or Special	
A-1		

TABLE OF CONTENTS

I. INTRODUCTION AND FORMULATION

An important application of the wing-body juncture problem is in the study of the horseshoe vortex which occurs in the vicinity of a wing/strut-wall intersection for instance. Numerous flow visualization studies (Thwaites 1960, Baker 1979, Barber 1978, Thomas 1987) have shown that the horseshoe vortex system consists of a three-dimensional boundary-layer separation in front of the wing/strut followed by a vortex flow which wraps around the structure. This vortical flow is characterized by three-dimensionality, unsteadiness, and large Reynolds number but having viscous effects which are crucial to the flow evolution. Such flows exist in many situations. For example, horseshoe vortex flow occurs near the junction of an airplane wing with the fuselage (Thwaites 1960) or the junction of plate and support in a plate heat exchanger. Another example is present in axial turbomachinery (Barber 1978) where boundary layers which develop on the annular surfaces of the axial flow passage encounter rows of stationary and rotating blades. The horseshoe vortical flow is of engineering interest because it can lead to flow degradation, high wall shear stresses, and high local heat transfer rates. It also plays a role in the origin of three-dimensional corner flows.

Three-dimensional fluid motion past a wing-body juncture or the related problem of corner flow is of fundamental importance in fluid mechanics as noted above. In all of these cases, the concern is with both the local and global scales of the viscous

forces produced by the body as well as with any significant
secondary flows which may be set up. It is hoped that an
understanding of these types of flows and their scales will
provide us with a more complete understanding of complicated
three-dimensional, high Reynolds number flows. To this end, the
concepts of interaction theory have been utilized with the
ultimate goal of elucidating the major effects of viscosity and
heat transfer on the local flowfield near a wing-body juncture
for subsonic mainstream flows.

Smith & Gajjar (1984) were the first to consider the problem
of a steady, incompressible, laminar flow past a juncture made up
of a localized small-scale thin wing protruding from a locally
flat surface when the Reynolds number, Re, is large, using the
triple-deck theory of viscous-inviscid interactions. A schematic
of the geometry considered by these authors and that to be
considered in this report is shown in Figure 1. Smith & Gajjar's
theory was developed to accommodate small wings of finite span
which scale with the streamwise and spanwise triple-deck length
scales. However, as was determined as part of this current
research effort, Smith & Gajjar's theory is not generally
applicable to all suitably scaled wing shapes, as will be
discussed below. The incident boundary layer on the body surface
is assumed to be driven by a locally uniform external flow and it
is taken to be well developed, attached, and planar in character.
Under these conditions an interaction between the body surface
flow and the wing is established which presumably has the triple-

deck structure wherein the motion past the thin wing provokes on the body surface an unknown pressure force which interacts with the unknown displacement thickness there. Due to this interaction, the boundary layer on the body surface becomes three-dimensional and exhibits upstream influence. Furthermore, a nonlinear interaction is possible if the slope of the thin wing in the interaction region is of the order $Re^{-1/4}$.

As shown by Smith & Gajjar (1984) the fundamental problem, as sketched in Figure 1, can be reduced to a consideration of the following boundary-value problem for an incompressible steady flow in terms of suitably scaled velocity components (U,V,W), pressure, P(X,Y), and displacement thickness function, δ(X,Y), in the (X,Y,Z) directions, respectively. More complete details of the scaling laws and the triple-deck nature of the flowfield structure can be found in Lee (1994). The fundamental governing equations appropriate for the viscous layer in the usual triple-deck theory are given by

$$\frac{\partial U}{\partial X} + \frac{\partial V}{\partial Y} + \frac{\partial W}{\partial Z} = 0 \tag{1}$$

$$U\frac{\partial U}{\partial X} + V\frac{\partial U}{\partial Y} + W\frac{\partial U}{\partial Z} = -\frac{\partial P}{\partial X} + \frac{\partial^2 U}{\partial Z^2} \tag{2}$$

$$U\frac{\partial V}{\partial X} + V\frac{\partial V}{\partial Y} + W\frac{\partial V}{\partial Z} = -\frac{\partial P}{\partial Y} + \frac{\partial^2 V}{\partial Z^2} \tag{3}$$

In addition, the following boundary conditions apply

$$U = V = W = 0 \quad \text{on } Z = 0, \tag{4}$$

$$U \to Z - \delta((X,Y), \quad V \to 0 \quad \text{as } Z \to \infty, \tag{5}$$

$$(U,V,W,P) \to (Y,0,0,0) \quad \text{as } |X| \to \infty, \tag{6}$$

and, and according to Smith & Gajjar (1984), the symmetry condition

$$V = 0 \quad \text{on } Y = 0. \tag{7}$$

The problem is closed mathematically by applying the pressure-displacement thickness interaction law, viz,

$$P(X,Y) = -\frac{1}{\pi}\int_{-\infty}^{\infty}\frac{df}{d\xi}(\xi)\frac{X-\xi}{(X-\xi)^2+Y^2}d\xi$$
$$+ \frac{1}{2\pi}\int_{-\infty}^{\infty}\int_{-\infty}^{\infty}\frac{\partial^2\delta}{\partial\xi^2}(\xi,\eta)\frac{d\xi\,d\eta}{\sqrt{(X-\xi)^2+(Y-\eta)^2}} \tag{8}$$

for two-dimensional wings, or

$$P(X,Y) = \frac{1}{\pi}\int_{-\infty}^{\infty}\int_{0}^{\infty}\frac{\partial^2 g}{\partial\xi^2}(\xi,\theta)\frac{d\theta\,d\xi}{\sqrt{(X-\xi)^2+Y^2+\theta^2}}$$
$$\frac{1}{2\pi}\int_{-\infty}^{\infty}\int_{-\infty}^{\infty}\frac{\partial^2\delta}{\partial\xi^2}(\xi,\eta)\frac{d\xi\,d\eta}{\sqrt{(X-\xi)^2+(Y-\eta)^2}} \tag{9}$$

for three-dimensional wings, where hf(X) is the scaled local two-dimensional wing surface shape, while the three-dimensional wing surface is defined by hg(X,Y). We should note that it is the wing shape which generates the forcing which in turn generates the interaction and three-dimensionality in the body's boundary layer. This forcing comes from outside the boundary layer itself and is, therefore, quite different from the usual three-dimensional interactive flow produced by a small hump in a boundary-layer flow.

In general the problem posed in equations (1) - (7) and (8) or (9) above is nonlinear and thus requires a numerical treatment. However, Smith & Gajjar (1984) and Lee (1994) have considered linearized solutions of these equations, using Fourier transform methods, valid for small values of the wing thickness parameter h, and several choices for the wing shapes f(X) and g(X,Y).

These linearized results always showed two maximum local deficits occurring in the streamwise surface shear stress on the body, just ahead of and beyond the front of the wing, on the axis of symmetry, which suggests that a regular separation or flow reversal would tend to occur there first, when the flow is sufficiently nonlinear. This result, coupled with the corresponding spanwise surface shear stress patterns, led to qualitative agreement with experimental observations, as noted by Smith & Gajjar (1984), of a separation line starting upstream of the wing and bending around it, and of separation downstream. Furthermore, the secondary flow patterns found from the linearized analysis tend to tie in with those found in experiments also.

In view of the encouraging results of the linearized theory, in this research effort numerical solutions of the nonlinear boundary-value problem defined by equations (1) - (7), and (8) or (9) have been found for several wing shapes with the goal of determining, among other things, the conditions for boundary-layer separation. We have also extended the theory to include the

effects of temperature on the flow when the mainstream is
subsonic in character. Referring to Lee (1994) for details, it
can be shown that the energy equation in suitably scaled
variables for the nondimensional temperature distribution, T, in
the viscous sublayer is given by

$$U\frac{\partial T}{\partial X} + V\frac{\partial T}{\partial Y} + W\frac{\partial T}{\partial Z} = \frac{1}{Pr}\frac{\partial^2 T}{\partial Z^2} \tag{10}$$

along with the boundary conditions

$$T(X,Y,Z) \sim Z \; \text{ as } \; |X|,|Y| \to \infty$$
$$T(X,Y,0) = 0, \; T(X,Y,Z) \sim Z - \delta(X,Y) \; \text{ for } Z \to \infty \tag{11}$$

when we can assume that the wall temperature and Prandtl number,
Pr, are constants. It should also be noted that the above system
of equations is valid for *any* subsonic flow since all parameters
related to the compressibility effects of the flow can be scaled
out in the triple-deck formulation of the problem (see Lee 1994).

In obtaining numerical solutions to the linearized form of
the above equations for h << 1, Smith & Gajjar (1984) introduced
the concept of an "effective" hump shape to transform the
linearized physical wing-body juncture problem into an equivalent
three-dimensional hump-like problem using an appropriate
transformation relating the displacement thickness, interactive
pressure and the wing shape. This change allowed for rather
simple computations to be done using a finite-Fourier transform
method to convert the closed-form solutions for the pressure,
displacement thickness and wall shear stresses in spectral space

to equivalent functions in physical space. Lee (1994) confirmed these results and also computed the wall heat transfer distribution functions.

In our study of the linearized version of this problem it was determined that the theory developed by Smith & Gajjar is not generally applicable for the airfoils they used in their paper due to the imposition of symmetry conditions on the pressure and the spanwise velocity. These conditions are inconsistent with the physical formulation of the wing-body problem except for "wing" shapes, f(X), that are composed of linear elements, such as in a diamond shaped airfoil. This restriction places rather serious limits on the types of airfoils for which this theory is useful. It should be noted that attempts at generalizing this theory to include a broader class of wing shapes was not successful.

Of primary concern in this research effort was the numerical solution of the nonlinear governing equations (1) - (11) for acceptable wing shapes and order-one values of the wing shape parameter h. Two different approaches for the numerical scheme were considered. In one approach, the finite-difference method for three-dimensional interacting flows developed by Bodonyi & Duck (1988) wherein the pressure-displacement law, equation (8) or (9), is replaced by a numerical solution of the upper-deck boundary-value problem which is solved simultaneously, following the ideas originally proposed by Veldman (1979), along with the finite-difference form of equations (1) - (3). In previous studies this approach has proved to be quite useful in computing

three-dimensional nonlinear interacting flows. In the second approach the solution of the system (1) - (3) along with a numerical implementation of the Cauchy-Hilbert integral, (8) or (9), using Smith's approach (1991) to discretize the pressure-displacement, law was determined.

In either approach the above set of equations is elliptic in the pressure field and therefore requires a modification of the multi-sweep forward-marching methods which were successfully developed for 2-D problems. As noted by Smith (1983) this ellipticity causes an explosive 3-D free interaction in any forward-marching procedure unless treated properly. To overcome these difficulties, a skewed-shear method is used to cast the problem in a quasi-two-dimensional form (see Bodonyi & Duck 1988 and Lee 1994) while at the same time capturing the elliptic nature of the inverse 3-D boundary-layer problem. In terms of these new variables, a second-order finite-difference method was developed for the governing equations and numerical solutions of the finite-difference equations were computed for a variety of grid sizes and several choices for the wing shape. The computations are involved, requiring the use of the CRAY YMP/864 supercomputer at the Ohio Supercomputer Center. Results of the numerical computations are given in the following section.

II. NUMERICAL RESULTS

After considerable study, it was determined that the second numerical approach discussed above resulted in the most accurate solutions of the governing equations. Therefore, the numerical results to be presented below will be taken from that approach. As noted above, for the theory to be strictly applicable, the two-dimensional wing shape, $f(X)$, must be composed of linear elements. Thus we shall consider the diamond-shaped airfoil defined by

$$f(X) = \begin{cases} X & \text{for } 0 < X < 0.5 \\ 1-X & \text{for } 0.5 < X < 1 \end{cases} \tag{12}$$

The grid sizes used in all cases have 101 points for $-4.5 \leq X \leq 5.5$, 31 points for $0 \leq Y \leq 3.75$ and 41 points for $0 \leq Z \leq 6$ in the streamwise, spanwise and normal directions, respectively. The local convergence criterion for the interactive pressure and the global convergence criterion for the velocity components are 10^{-5} and 10^{-3}, respectively.

A surface plot of the effective hump shape generated by the diamond shaped airfoil is given in Figure 2. It is clearly evident that this "effective" hump shape is very peaked near $Y=0$ and $X = 1/2$. This sharp peak places severe limitations on what grid sizes are needed to adequately resolve the flow structure in this vicinity, and it is a primary reason that numerical solutions could be found only for rather limited ranges of the parameters involved. This situation is quite different than in the "regular" 3-D hump problem considered by others since in

those cases the hump shape could be more conveniently defined so that such situations as that noted above did not occur. In the current study the "hump" shape is predetermined, depending only on the actual wing shape and the mathematical transformation inherent in the problem.

Figures 3 through 6 give comparisons between the linearized solutions using the FFT method and the nonlinear solutions using the finite-difference method for small h. Note that the results are quite close to each other, indicating that the nonlinear finite-difference computational method developed in this effort does work. For completeness, Figures 7 - 11 give the surface plots for the pressure, stream and spanwise shear stress distributions, displacement thickness, and wall heat transfer distributions, obtained from the nonlinear computations for h=0.1.

Nonlinear solutions on the plane of symmetry, Y = 0, for various values of h are given next in Figures 12 - 15. Note that oscillations begin to appear in the solution for the pressure when h = 0.5, and they are clearly evident when h = 1.0. This numerical instability could not be removed from the computations, and this eventually prevented the computation of further solutions for larger values of h. Unfortunately, this numerical breakdown always occurred before separation on the body surface in front of the wing occurred. Also note that the nonlinear solutions at Y = 0 do not return to either 0 or constant values at the downstream limit of the computational domain. The reason

for this discrepancy is that the computational domain for the nonlinear problem is much smaller in extent than that for the linearized solutions found by the FFT method. Due to computer resource limitations it was not feasible to solve the nonlinear problem on larger domains, although it is believed that the computations would return to their appropriate values if a larger domain were utilized.

Figure 16 shows the flow streamlines in the plane of symmetry (Y = 0) and Figures 17 through 19 show the cross-flow streamlines near the leading edge, at mid-chord, and near the trailing edge for h = 0.5. Note that the directi ⌐ of the normal velocity is downward near the wing (0 < X < 1). This effect is indicated by the solid lines in Figures 17 and 18. However, the normal velocity changes sign near the trailing edge as shown by the dotted lines in Figure 19. The surface stress pattern for this problem is shown in Figure 20. The only noticeable effects on the surface due to the wing are in the vicinity of the wing (0 < X < 1, Y = 0).

The sharp peak of the effective hump at Y = 0 seems to be the main cause for the numerical difficulties which occur behind the wing. This sharp peak is the result of discontinuities in the derivative with respect to X of the wing-shape function which appears in the pressure-displacement thickness relationship. As noted without reaching large enough values of h it is impossible to have separation around the wing. For example, the flow over a "regular" hump shape $h \cdot \exp(-x^2-y^2)$, will result in boundary-layer

separation when h is approximately 2.8 (see Bodonyi & Duck 1988). Separation in front of this wing-body junction would be expected to occur for such order-one values of h. However, in this problem, the numerical scheme becomes unreliable for h > 0.5, and for these, or smaller, values of h, the flow near the surface is still strongly attached, precluding the possibility of bounc - layer separation.

For a study of step-size effects, an effective hump shape is computed for a finer grid with $\Delta X = 0.05$ and $\Delta Y = 0.0625$ for the diamond-shaped airfoil. Figure 21 shows the comparison of the effective hump shape for the two different meshes. The effective hump shape generated using this finer grid is input into the nonlinear wing-body solver using the grids $\Delta X = 0.1$ and $\Delta Y = 0.125$. In this case, the pressure shows oscillations for even smaller values of h than before, as shown in Figure 22. Much finer grids may therefore be needed along with wider ranges for each direction to increase h to larger values.

Linear and nonlinear solutions for a three-dimensional wing shapes of the following forms have also been computed:

$$g(X,Z_u) = f(X)[1 + \sigma Z_u] \tag{13}$$

$$g(X,Z_u) = \begin{cases} f(X - Z_u \tan\phi)e^{-\sigma Z_u} & \text{if } X > Z_u \tan\phi \\ 0 & \text{if } X < Z_u \tan\phi \end{cases} \tag{14}$$

Here $f(X)$ is the base shape of the wing adjoining the surface and Z_u is the upper-deck coordinate, ϕ is a sweep angle and σ is a

positive constant which controls the degree of tapering in the Z direction away from the body junction. The results of the computations are qualitatively similar to those of the two-dimensional wings discussed above and will not be repeated here. For further details on these three-dimensional solutions see Lee (1994).

III. CONCLUSIONS

In this research effort we have considered the flow structure near a small-scale wing-body combination within the framework of triple-deck theory. Thin airfoil theory was used to obtain the pressure distribution around a wing which in turn triggers a viscous-inviscid interaction near the wing-body juncture. As part of the formulation of the problem we have followed the lead of Smith & Gajjar (1984), utilizing the concept of an "effective hump shape" in the formulation of the nonlinear problem. This technique not only simplifies the pressure expression but also enhances the convergence of the numerical scheme even though the concept itself is just a transformation to convert the wing-body problem into a more conventional problem for computational efficiency.

As noted earlier, there is an important inconsistency in Smith & Gajjar's paper on the wing-body problem. According to the triple-deck scalings, the wing's presence enters in the upper deck of the triple-deck theory as a thin-airfoil formulation to leading order. In the lower-deck region, however, the only effect of the wing's presence is felt in the pressure field. Thus it can be shown that the boundary condition on the pressure must be given by

$$\frac{\partial P}{\partial Y}(X, Y=0) = -h\frac{d^2 f}{dX^2} \tag{15}$$

However, Smith & Gajjar omitted this condition and used $\partial P/\partial Y = 0$ instead. This is equivalent to taking the spanwise velocity, V,

equal to zero at the line of symmetry, and this is inconsistent for this problem. As a result it can be proved from the linearized problem that there can be no viscous-inviscid interaction for general two-dimensional wing shapes. Furthermore, this result seems to carry over to the nonlinear computations. The exception to this result occurs for wings composed of linear elements since in this case $f''(X)$ is identically zero. We note here that there can be a viscous-inviscid interaction for a three-dimensional wing shape as discussed in Lee (1994).

It is not clear at this point whether the triple-deck structure can accommodate interactions which originate outside the lower-deck region as originally noted by Stewartson (1974). Indeed, the results of this study suggest that the wing-body juncture problem is generally not of the triple-deck kind proposed by Smith & Gajjar, due to the inconsistencies in matching the solutions between the three regions of the flow field normal to the surface. In particular, the effects of normal pressure cannot be ignored, and the wing's presence must come into play in a more significant way than originally proposed. Unfortunately, attempts at developing such a theory have not been successful.

IV. PUBLICATIONS & PERSONNEL

Under the auspices of this research grant, one Ph.D thesis has been completed:

Lee, E.Y., 1994 "A Numerical Study of the Small Scale Wing-Body Junction Problem", Ph.D Thesis, The Ohio State University

The following personnel have participated in this research grant:

R.J. Bodonyi, Professor, The Ohio State University, Principal Investigator.

E.Y. Lee, Graduate Research Associate, The Ohio State University. Mr. Lee will receive his Ph.D degree at the end of the Winter Quarter, 1994.

V. REFERENCES

Baker, C.J. 1979, *J. Fluid Mech.*, V. 95, 347.

Barber, T.J. 1978, *J. Aircraft*, V. 15.

Bodonyi, R.J. & Duck, P.W.D. 1988, *Comput. Fluids*, V. 16, 279.

Lee, E.Y. 1994, Ph.D Thesis, The Ohio State University.

Smith, F.T. 1983, UTRC Report 83-46, United Technologies Research Center.

Smith, F.T. 1991, *Comput. Fluids*, V.20, 243.

Smith, F.T. & Gajjar, J. 1984, *J. Fluid Mech.*, V. 144, 191.

Stewartson, K. 1974, *Adv. in Appl. Mech.*, V. 14, 145.

Thomas, A.S.W. 1987, *Phys. Fluids*, V. 30.

Thwaites, B. 1960, Incompressible Aerodynamics, Oxford University Press, London.

Veldman, A.E.P. 1979, NLR-TR-79023. Dutch Nat. Aerosp. Lab., the Netherlands.
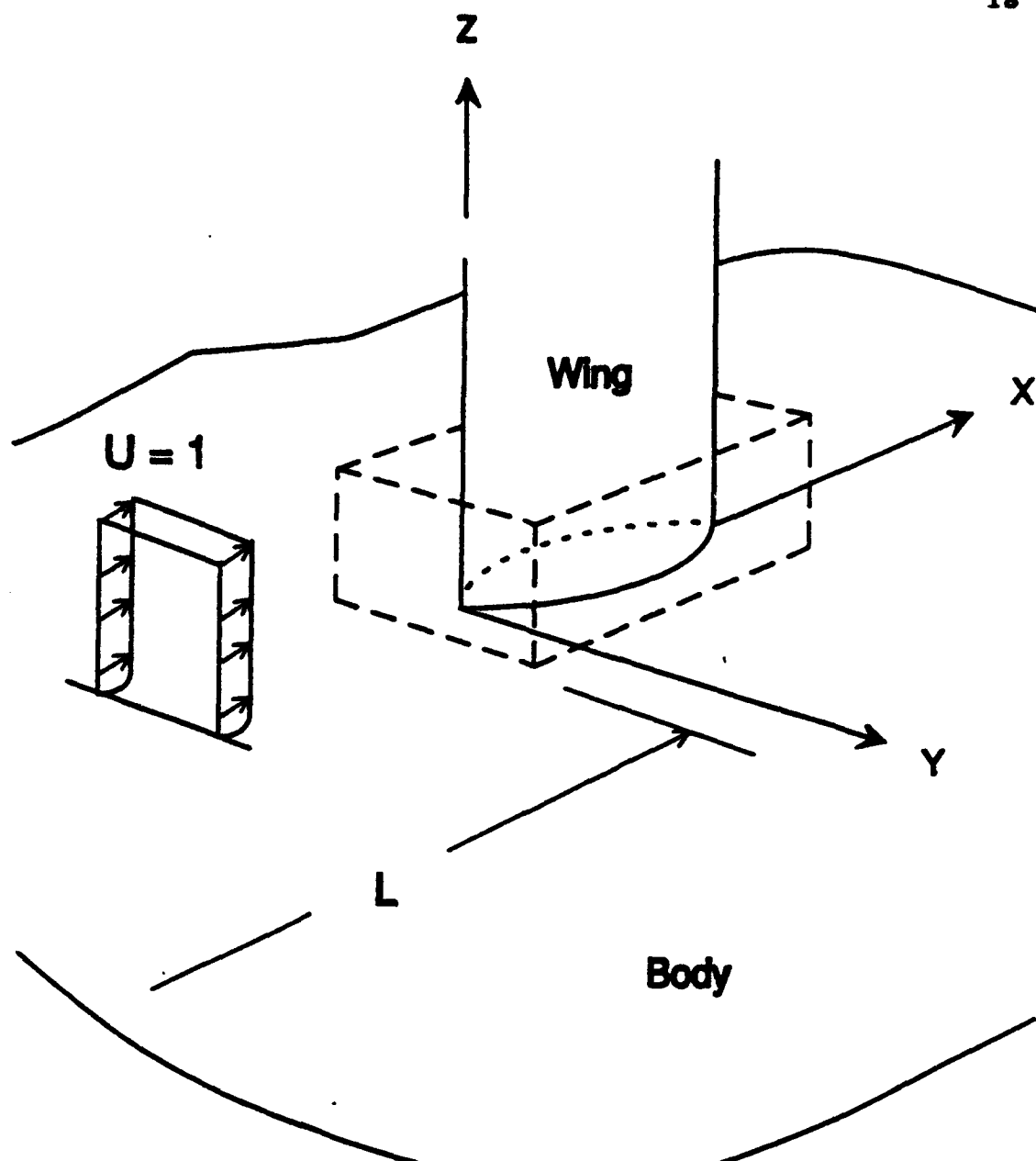
Figure 1: The triple-deck "box" describing the three-dimensional flow about the entire junction of a thin symmetric wing is shown by dashed lines. The box's dimensions are $O(Re^{-3/8}) \times O(Re^{-3/8}) \times O(Re^{-5/8})$ in the X,Y, and Z directions, respectively, and the distance to the box from the leading of the flat plate is $L = O(1)$.
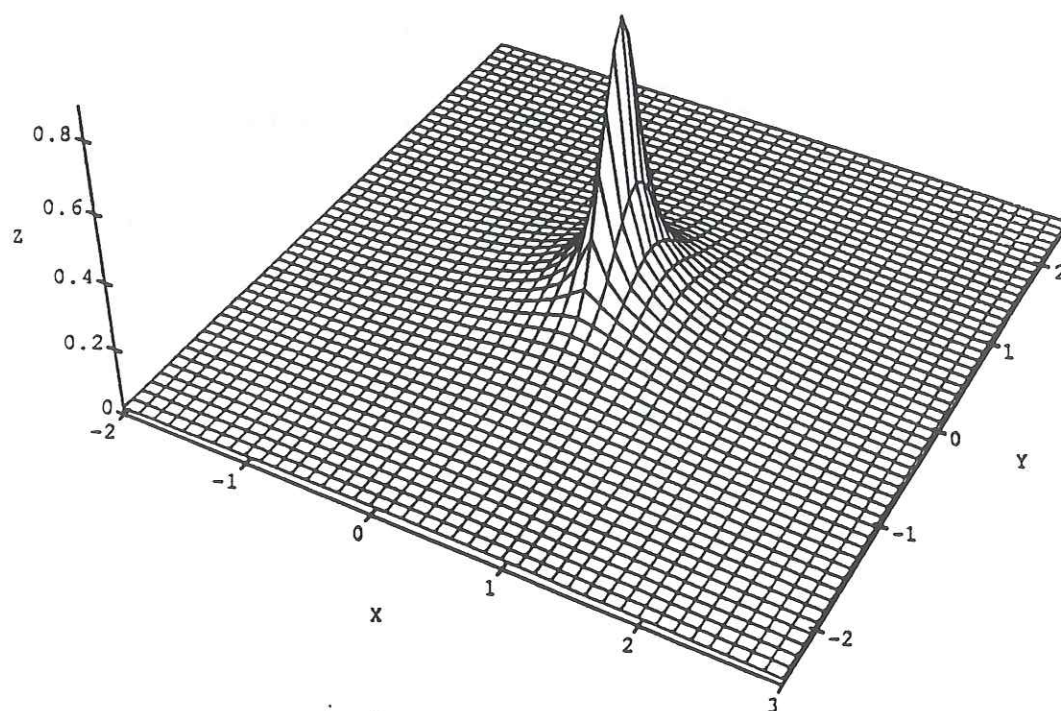
Figure 2: The effective hump shape generated by the two-dimensional wing for a diamond-shaped airfoil.
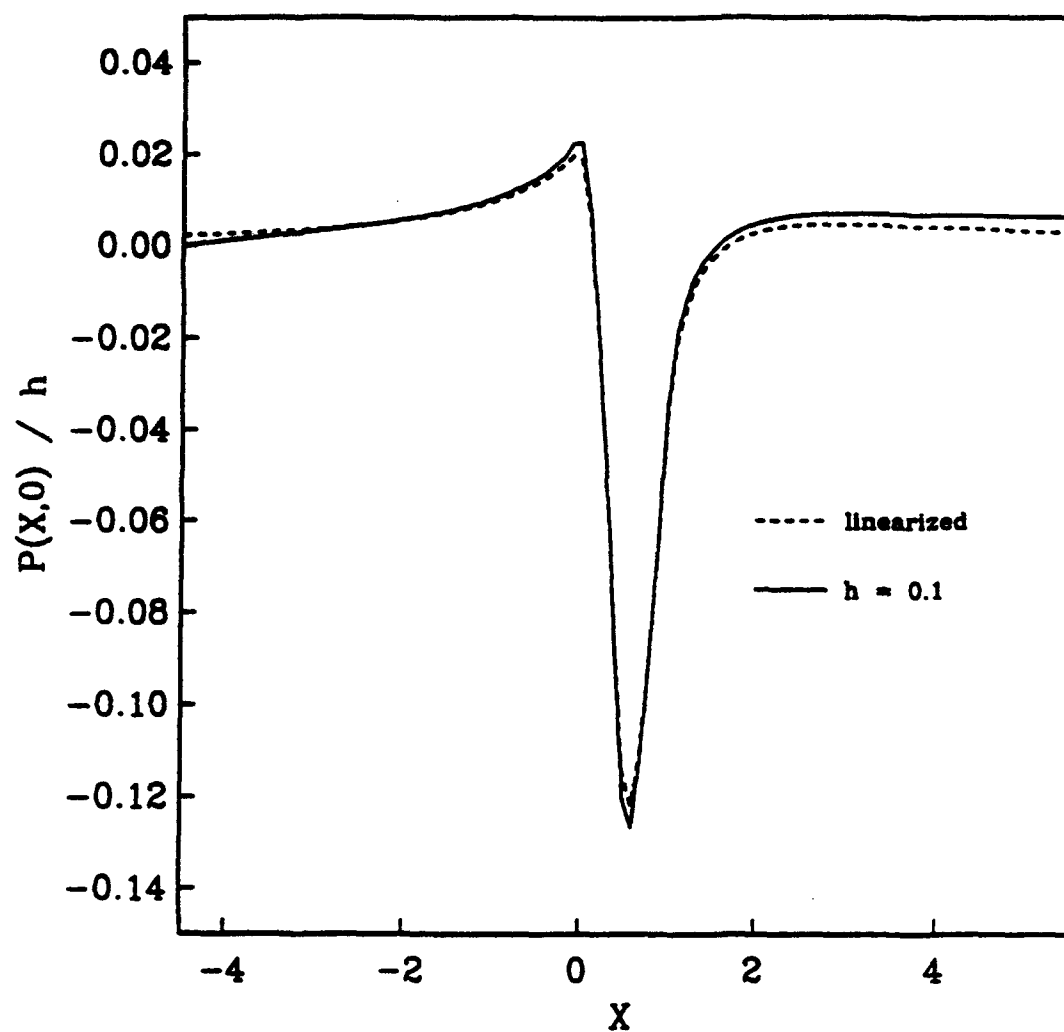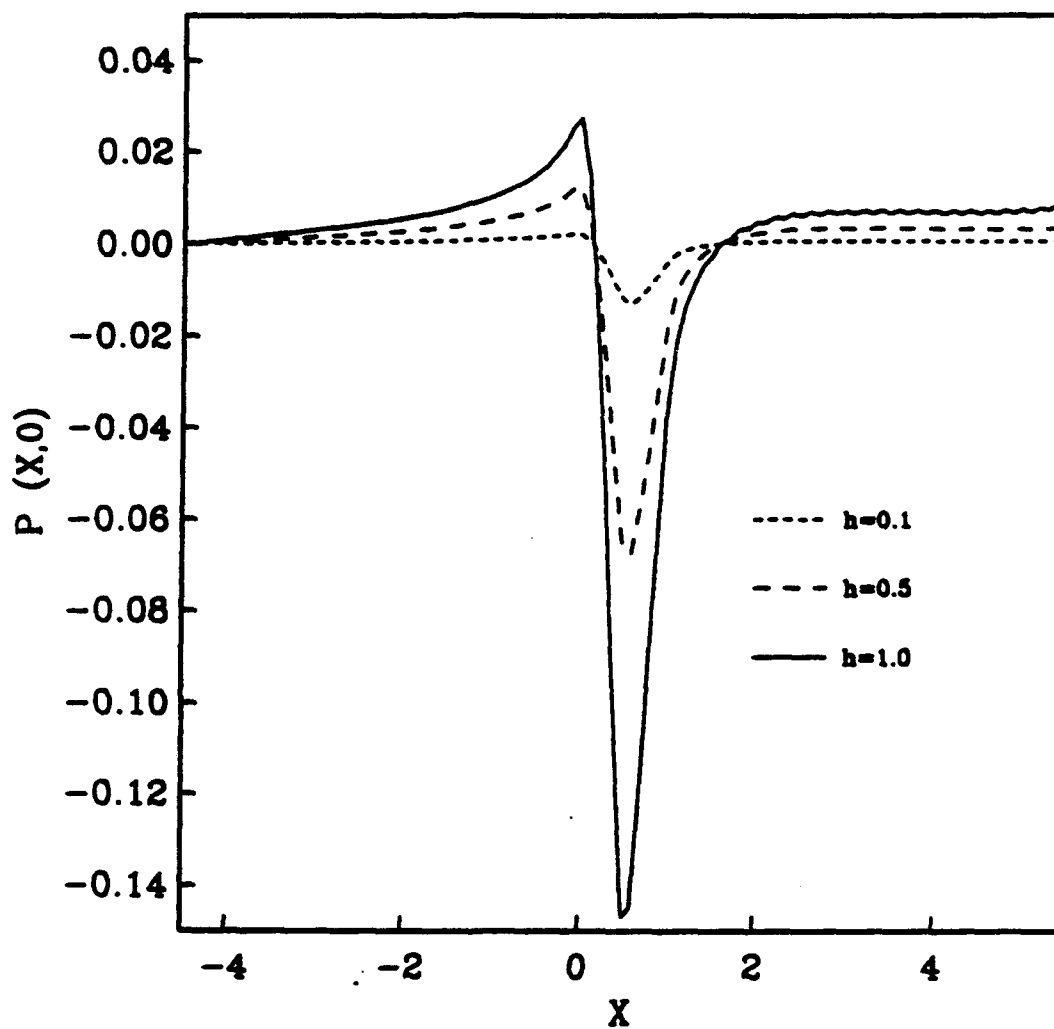
Figure 3: Comparison of surface pressures for linearized and nonlinear solutions of the two-dimensional wing-body for a diamond-shaped airfoil.
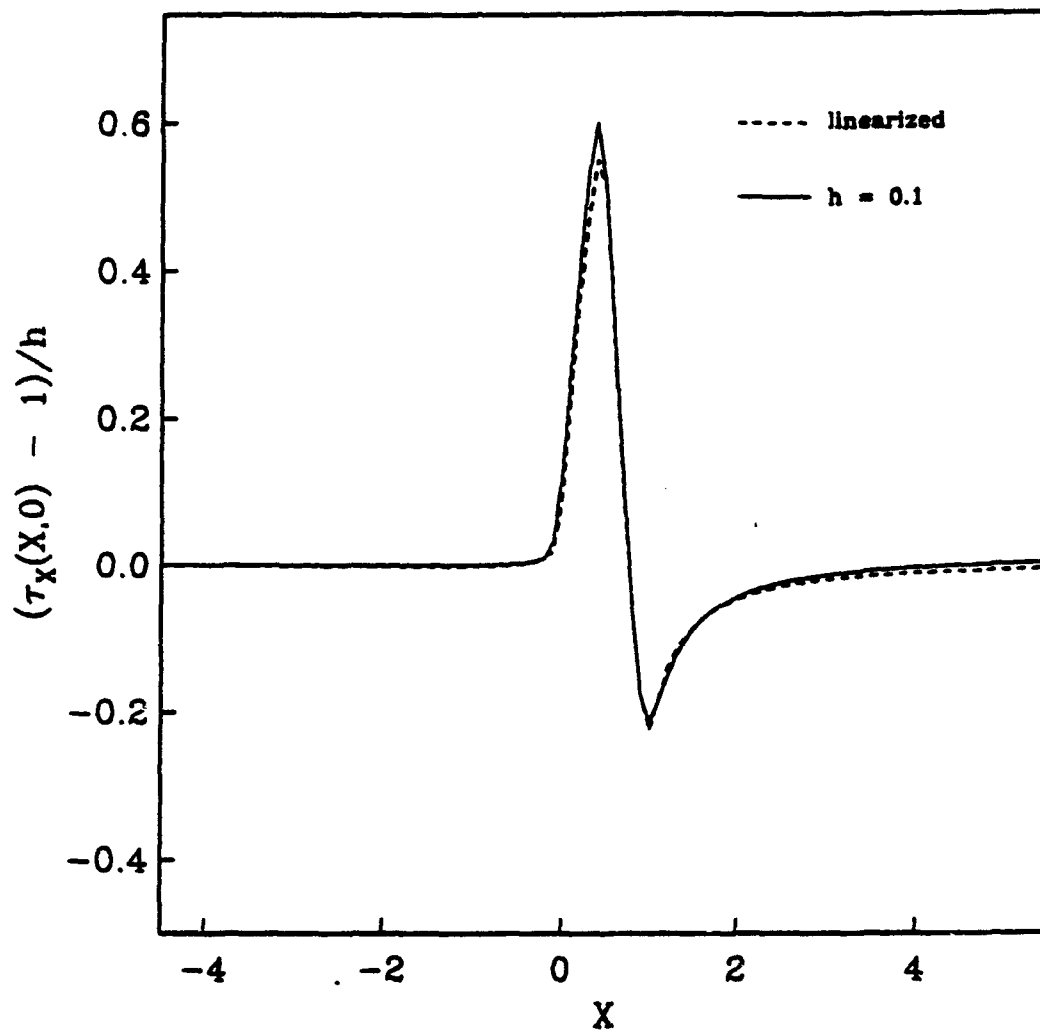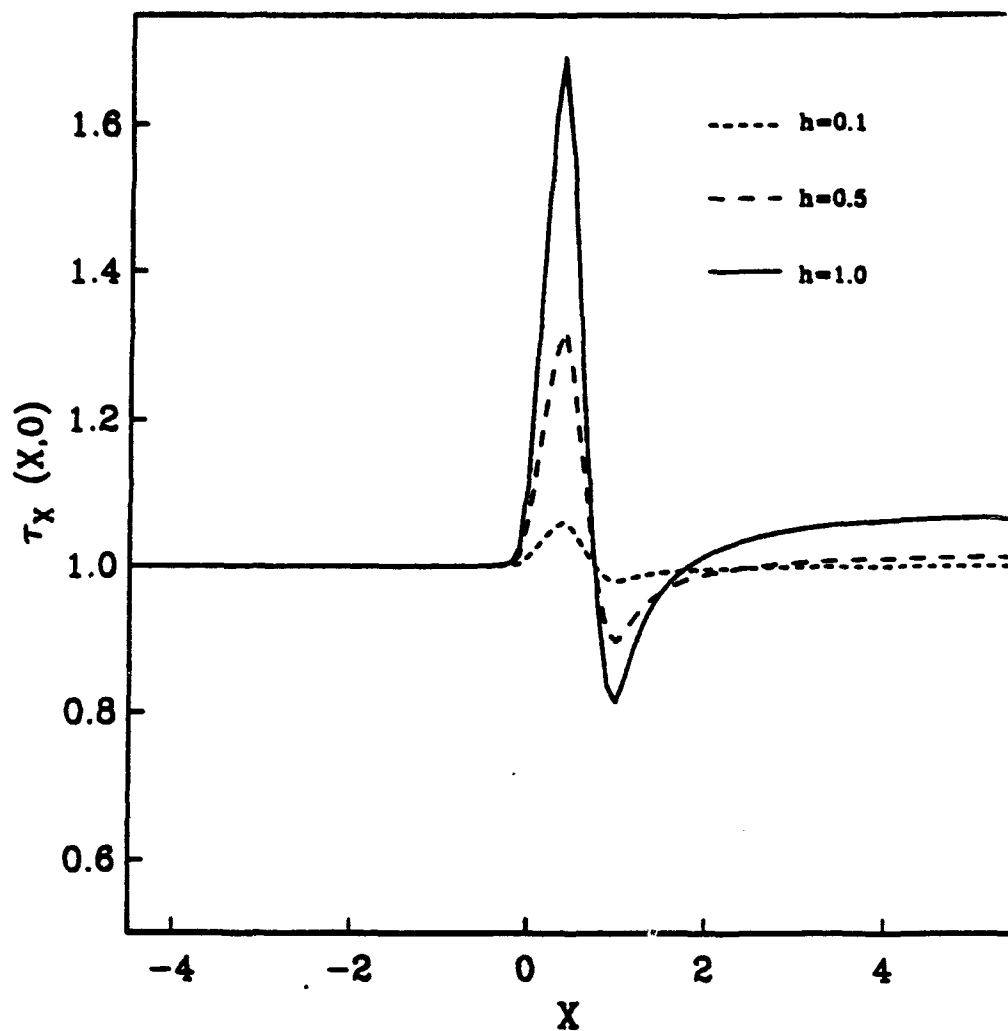
Figure 4: Comparison of streamwise shear stress for
linearized and nonlinear solutions of the
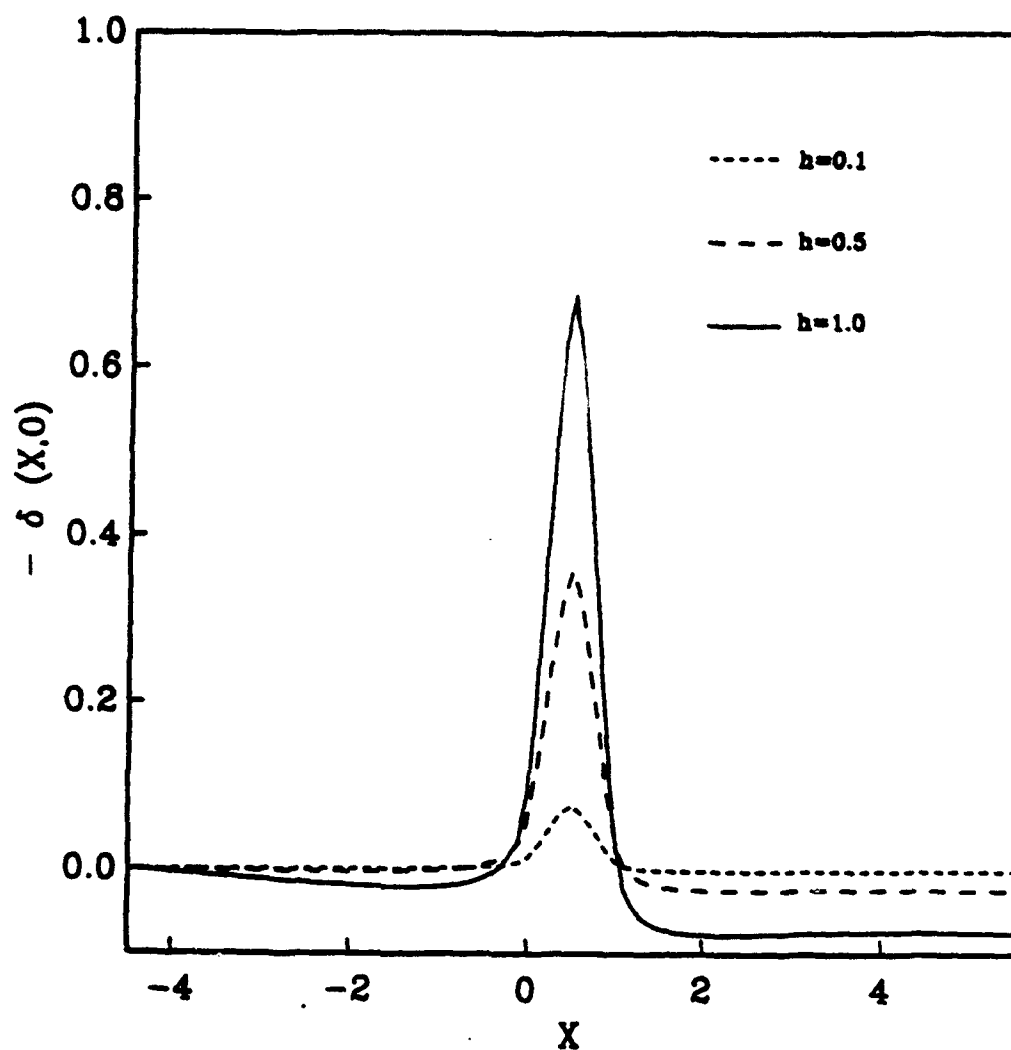two-dimensional wing-body for a diamond-
shaped airfoil.
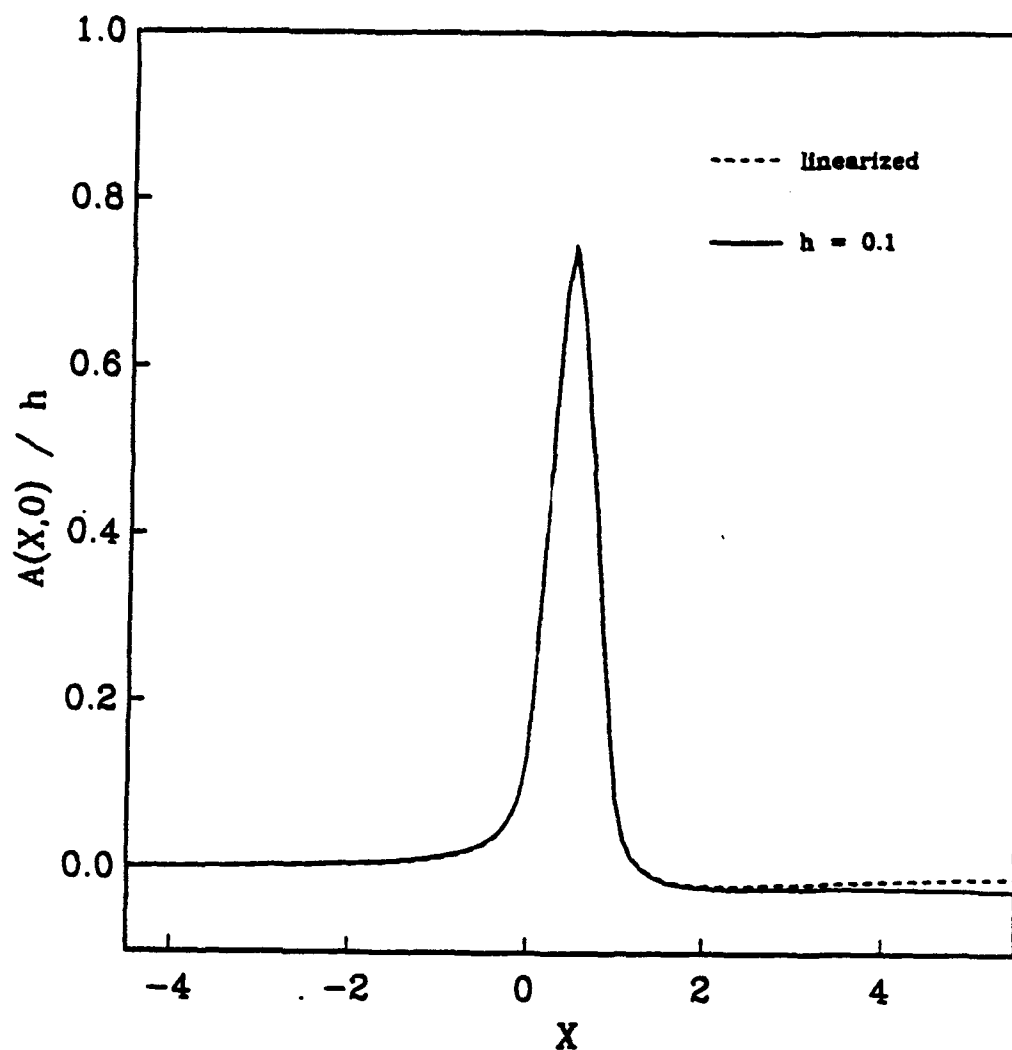
Figure 5. Comparison of displacement thickness for
linearized and nonlinear solutions of the two-
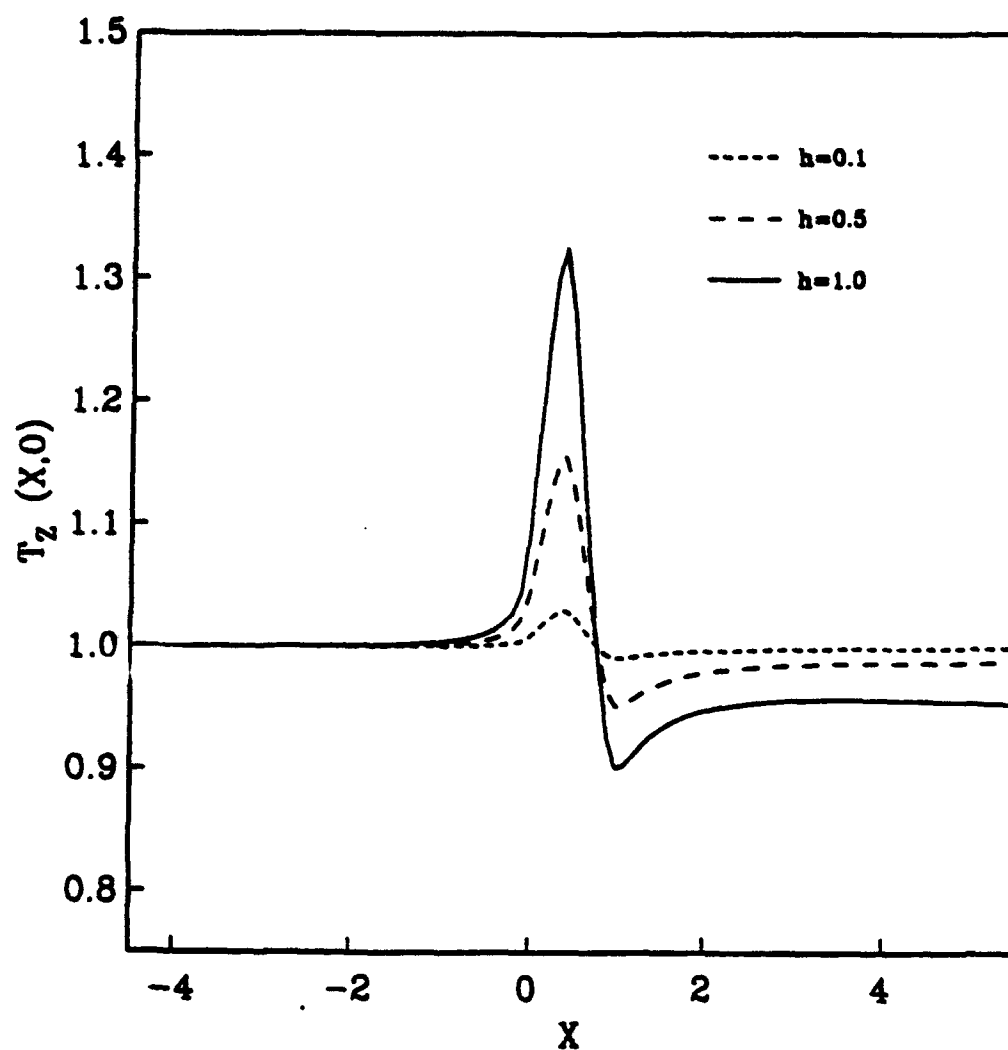dimensional wing-body for a diamond-shaped
airfoil.
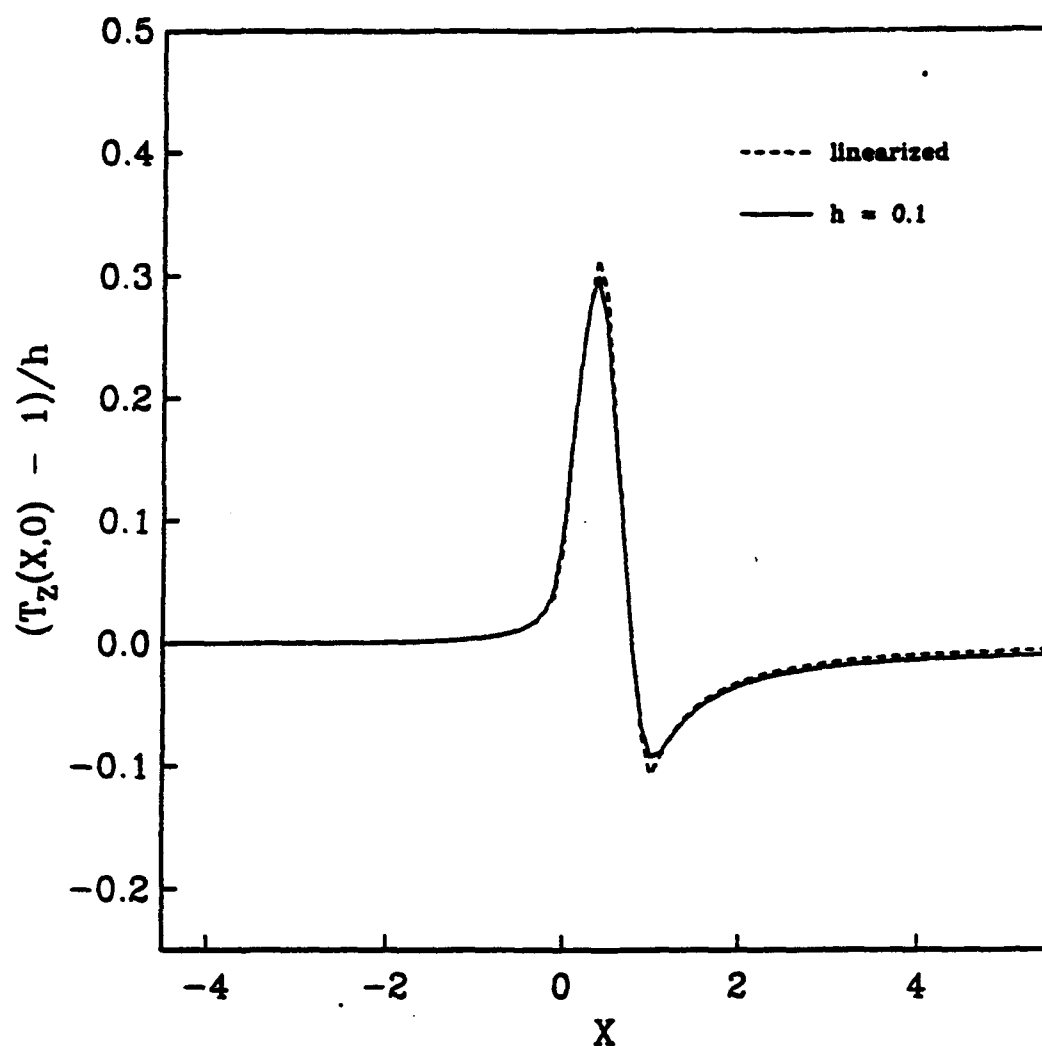
Figure 6. Comparison of wall heat transfer for linearized
and nonlinear solutions of the two-dimensional
wing-body for a diamond-shaped airfoil.
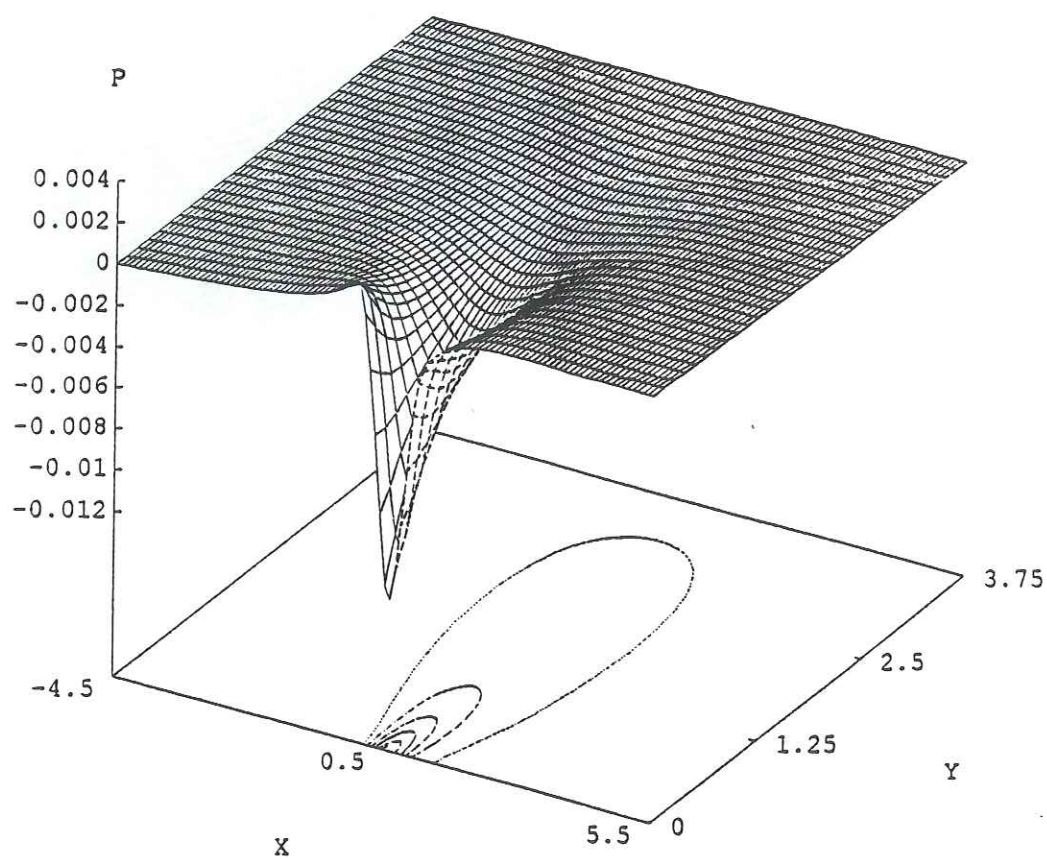
Figure 7: Surface pressure distribution for nonlinear flow (h = 0.1) of the two-dimensional wing-body for a diamond-shaped airfoil.
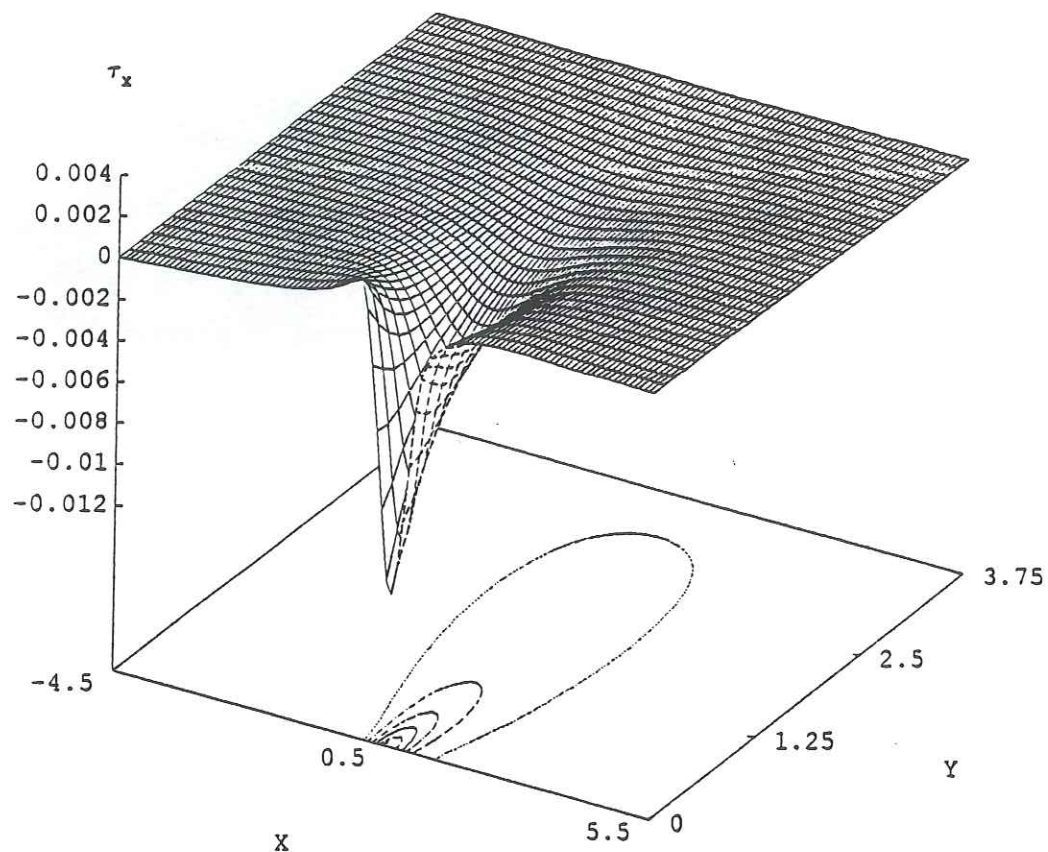
Figure 8: Streamwise shear stress distribution for nonlinear flow (h = 0.1) of the two-dimensional wing-body for a diamond-shaped airfoil.
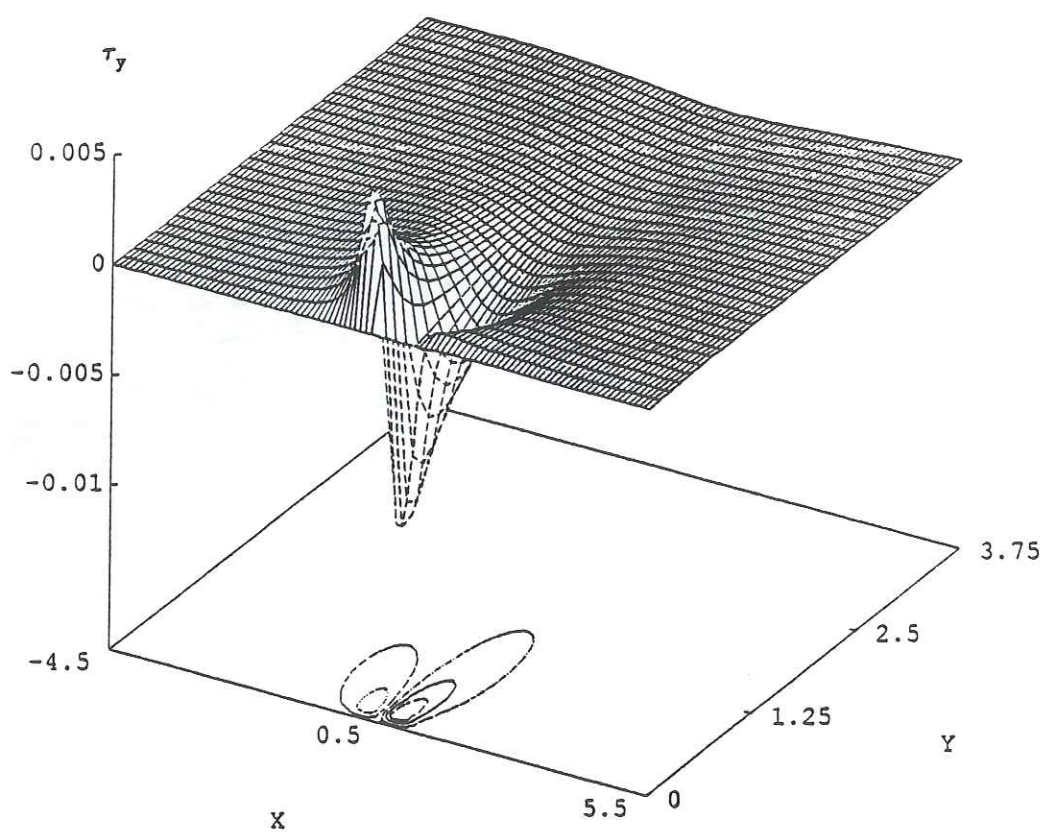
Figure 9: Spanwise shear stress distribution for nonlinear
flow (h = 0.1) of the two-dimensional wing-body
for a diamond-shaped airfoil.

$- \delta$
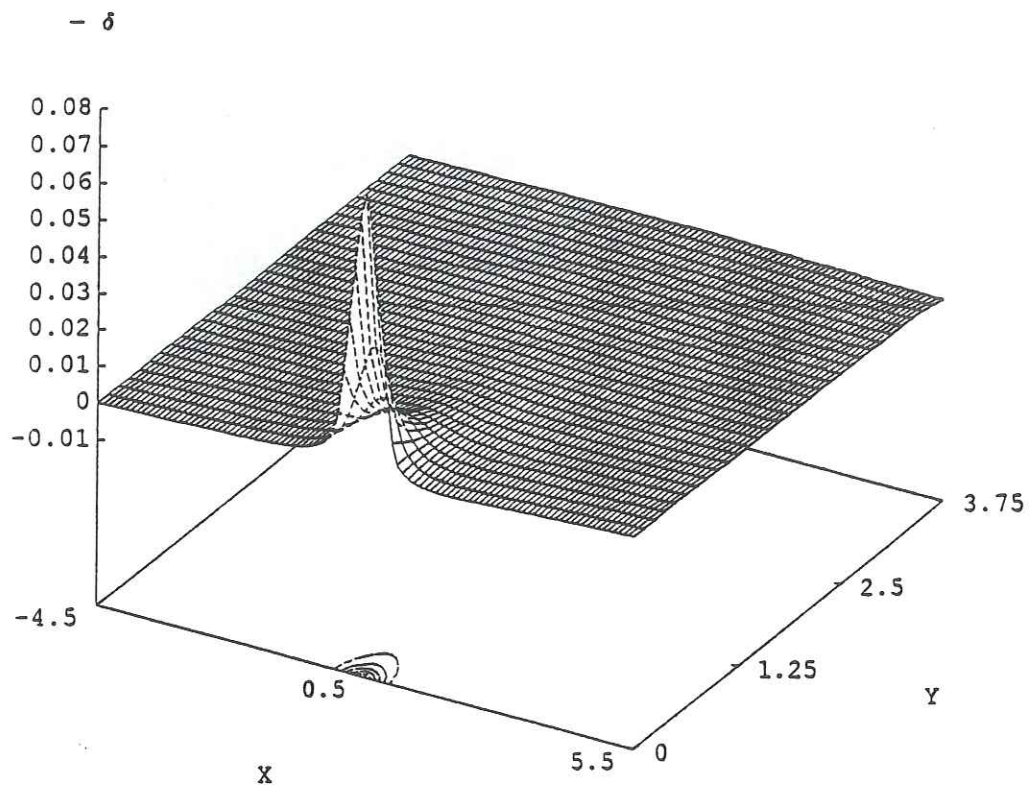
Figure 10: Displacement thickness distribution for nonlinear
flow (h = 0.1) of the two-dimensional wing-body
for a diamond-shaped airfoil.
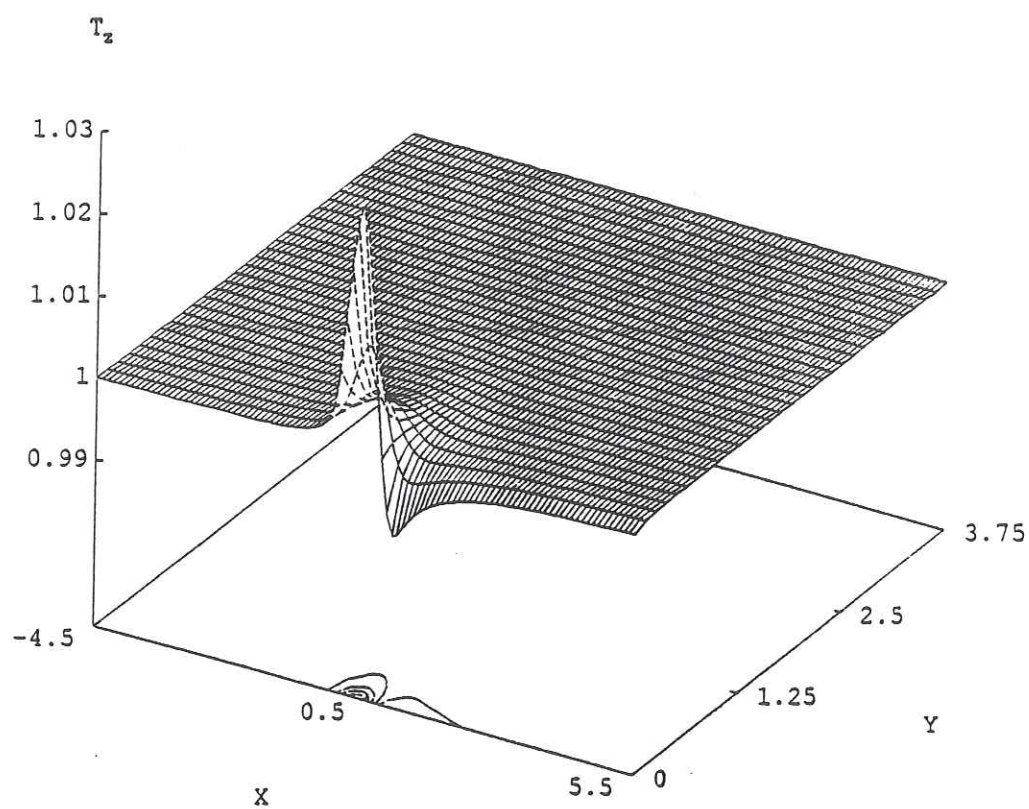
Figure 11: Wall heat transfer distribution for nonlinear
flow (h = 0.1) of the two-dimensional wing-body
for a diamond-shaped airfoil.

Figure 12: Comparison of surface pressures for nonlinear solutions of the two-dimensional wing-body for a diamond-shaped airfoil.

Figure 13: Comparison of streamwise shear stress for nonlinear solutions of the two-dimensional wing-body for a diamond-shaped airfoil.

Figure 14: Comparison of displacement thickness for nonlinear solutions of the two-dimensional wing-body for a diamond-shaped airfoil.

Figure 15: Comparison of wall heat transfer for
nonlinear solutions of the two-dimensional wing-
body for a diamond-shaped airfoil.
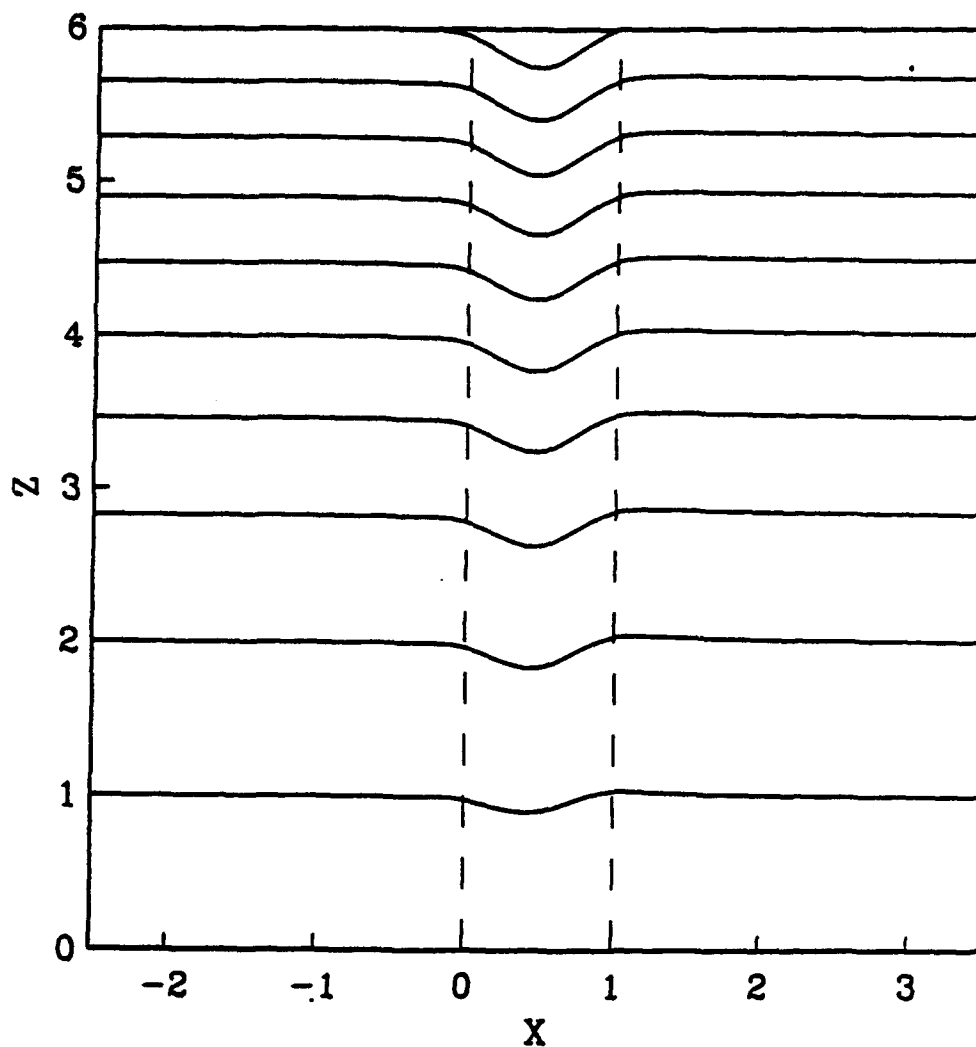
Figure 16: Flow streamlines in the plane of symmetry (Y = 0) for the two-dimensional wing-body for a diamond-shaped airfoil (h = 0.5, 0 < X < 1). The dotted lines indicate the location of the wing. The contour values are 0 (Z = 0), 0.5, 2.0, 4.0, 6.0, 10.0, 12.0, 16.0 and 18.0.
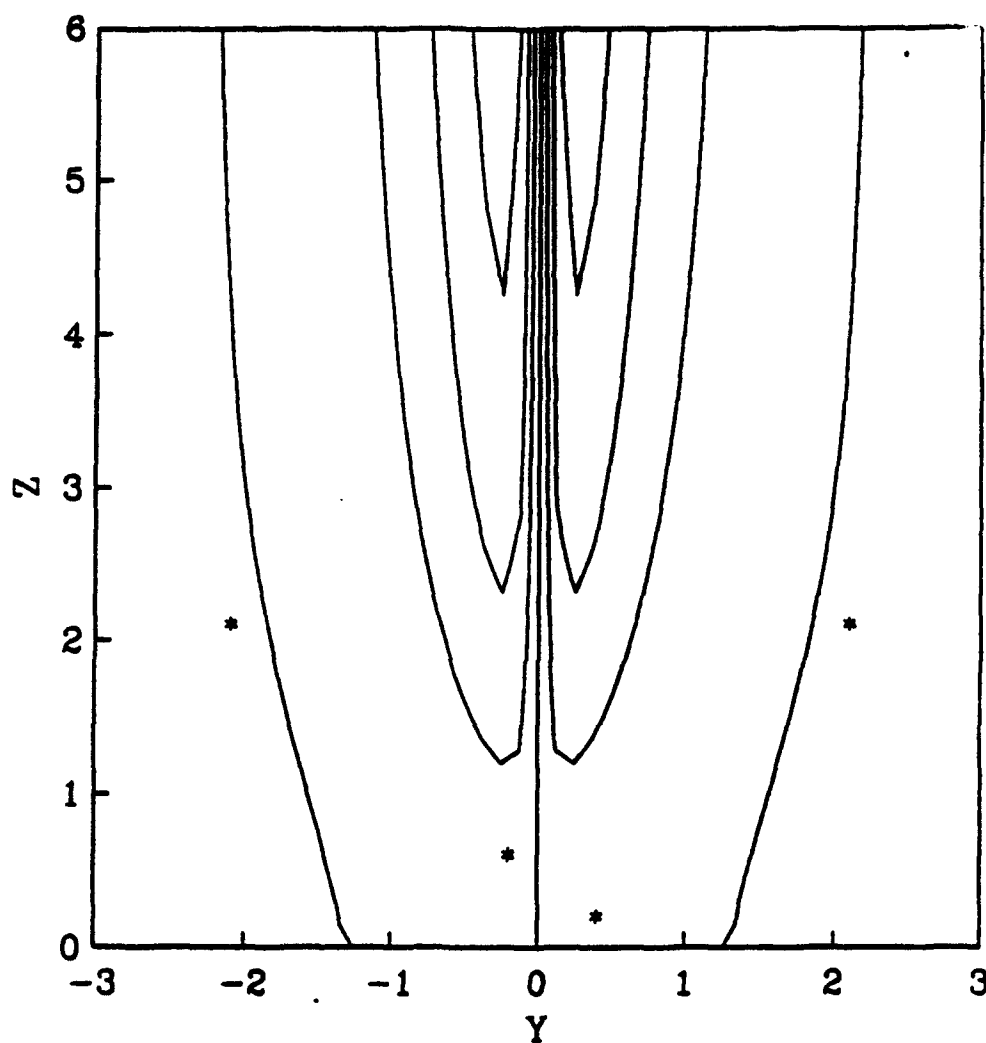
Figure 17: Cross-flow streamlines near the leading edge (X = 0) of the two-dimensional wing for a diamond-shaped airfoil (h = 0.5). The contour values are 0 (*), 0.01, 0.02, and 0.03.
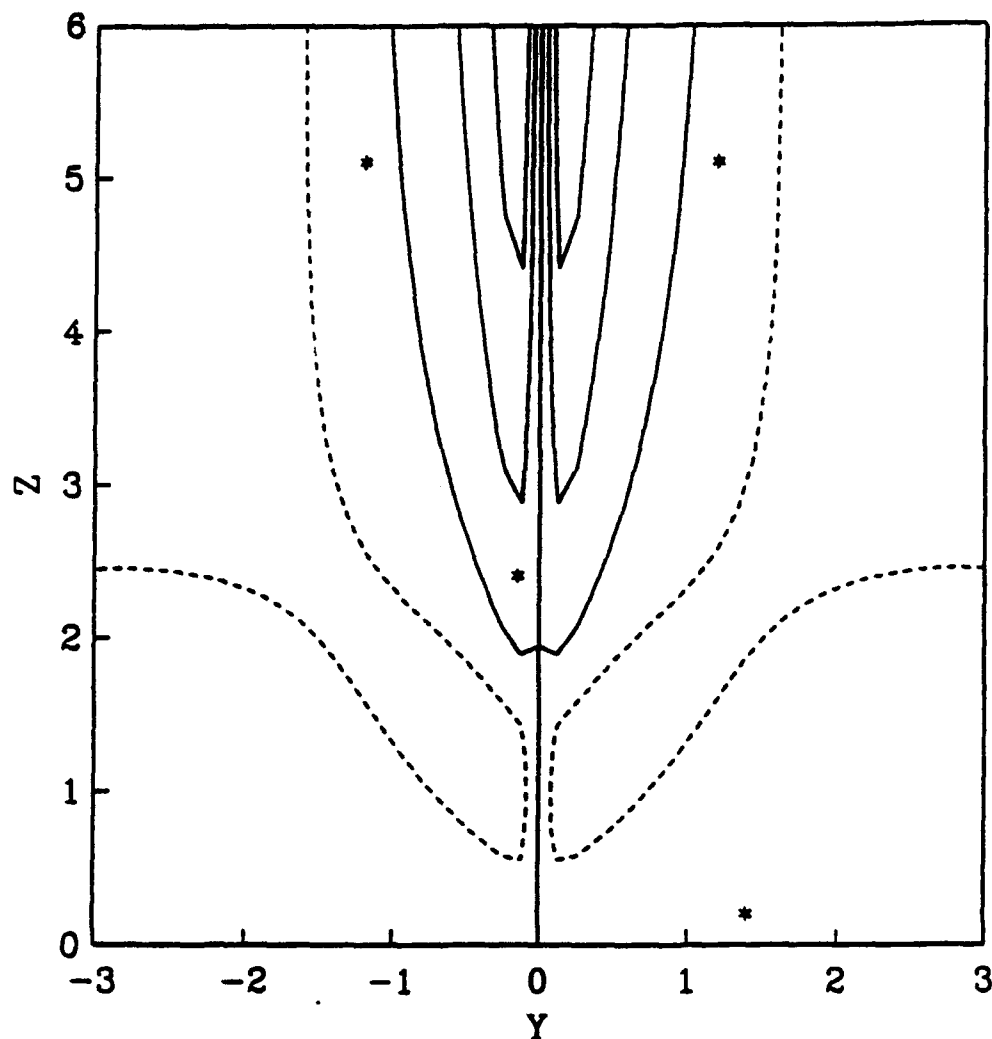
Figure 18: Cross-flow streamlines at the mid-cord (X = 0.5) of the two-dimensional wing for a diamond-shaped airfoil (h = 0.5). The contour values are -0.0025,0(*), 0.0005, and 0.01.
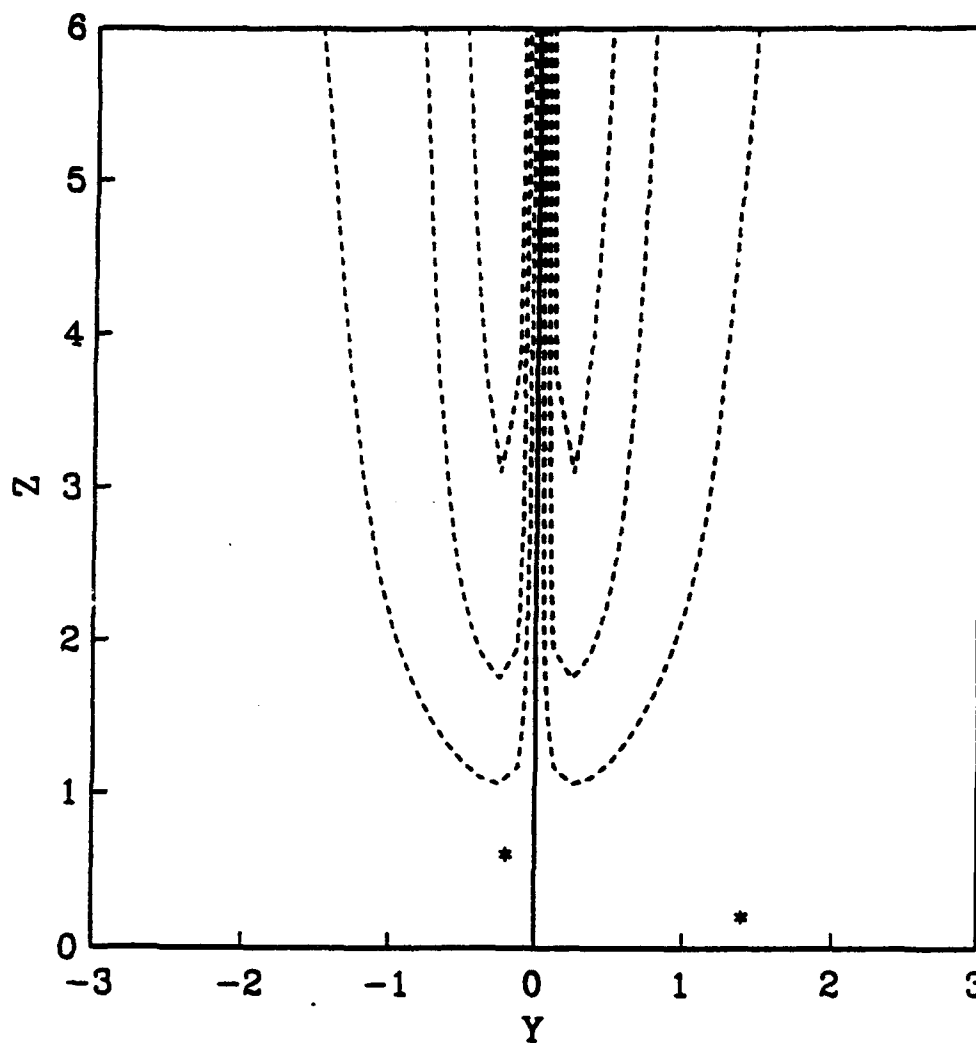
Figure 19: Cross-flow streamlines near the trailing edge (X
= 1) of the two-dimensional wing for a diamond-
shaped airfoil (h = 0.5). The contour values are
-0.003, -0.02, -0.01 and 0(*).

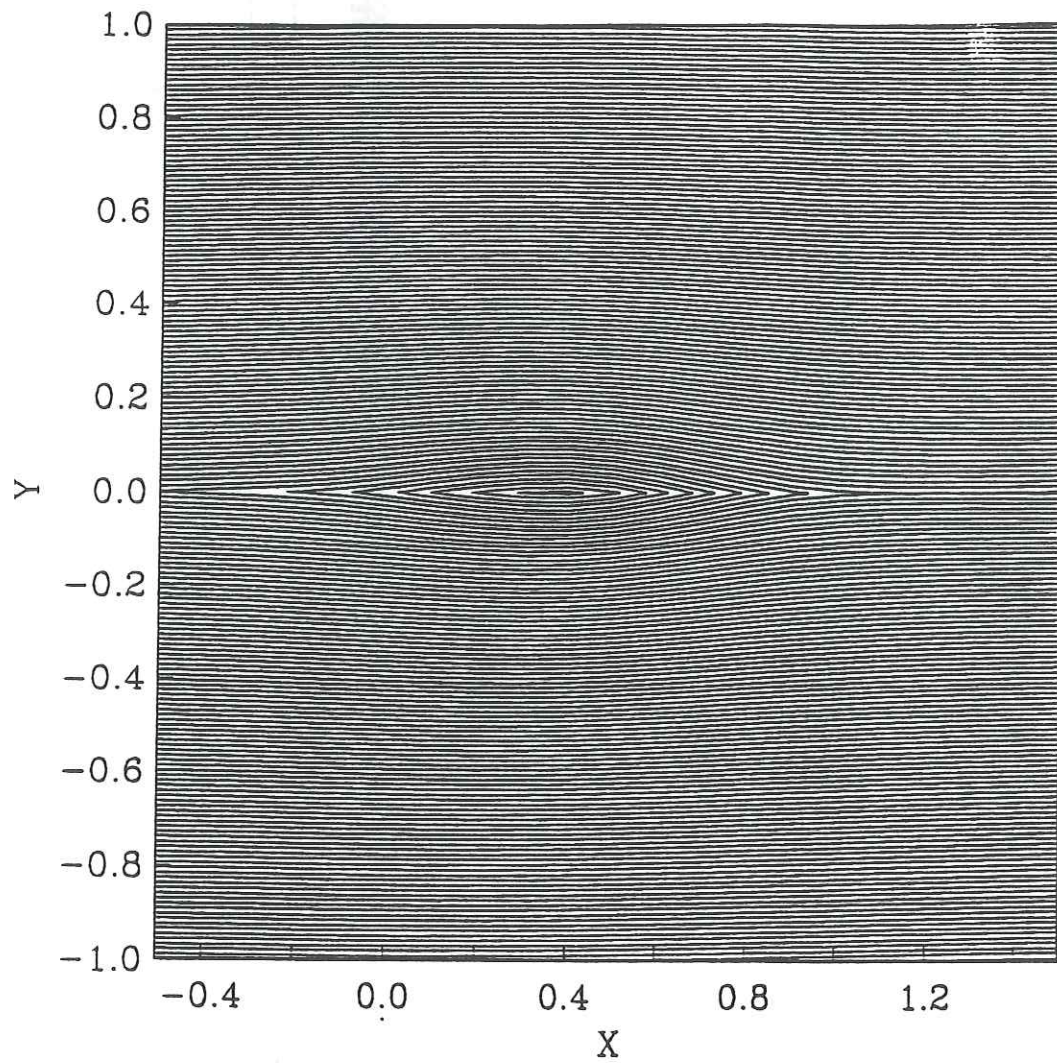Figure 20: Surface stress pattern for the two-dimensional wing-body for the diamond-shaped airfoil (h=0.5, 0 < X < 1).
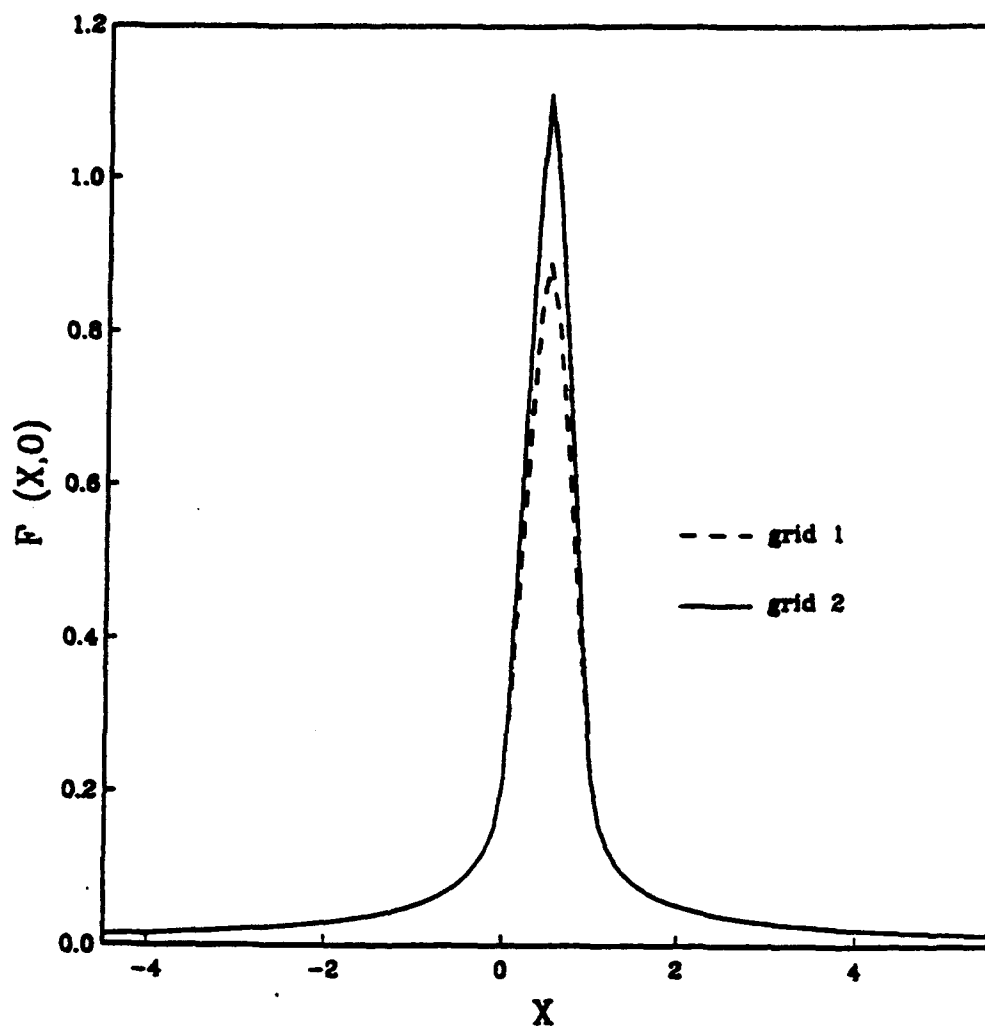
Figure 21: Comparison of effective hump shapes for the two-dimensional wing for the diamond-shaped airfoil (grid 1: $\Delta X=0.1$ and $\Delta Y=0.125$, grid 2: $\Delta X=0.05$ and $\Delta Y=0.0625$).
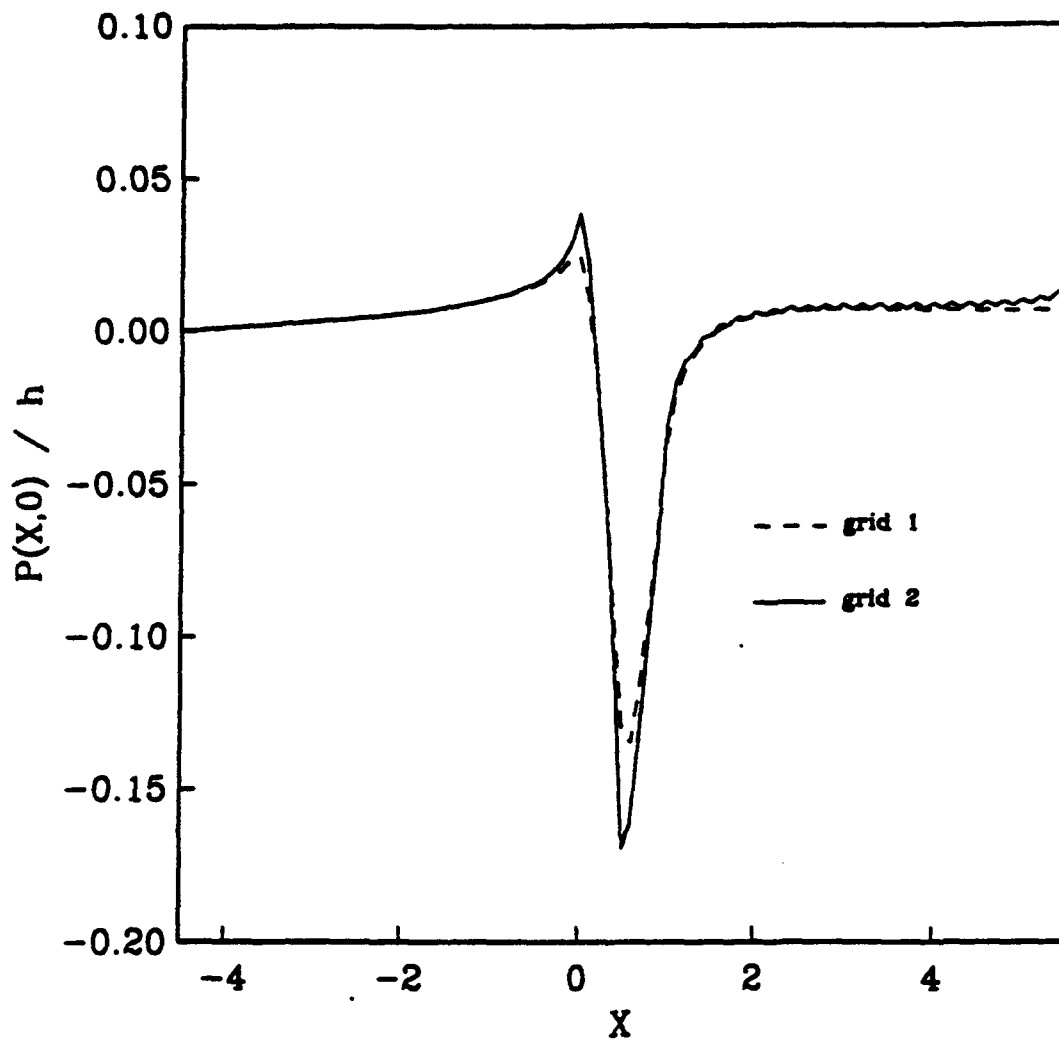
Figure 22: Comparison of surface pressures for nonlinear
solutions (h=0.5) for the two-dimensional wing
for the diamond-shaped airfoil (grid 1: ΔX=0.1
and ΔY=0.125, grid 2: ΔX=0.05 and ΔY=0. 0625).